Numerical Simulations in Cosmic Gas Dynamics —Gas Flows in Binary Stars—

By

Takuya MATSUDA*

(January 10, 1985)

Summary: Examples of numerical simulation in cosmic gasdynamics, i.e. gas flows in close binary stars, are presented. The first example is a calculation of Roche lobe overflow in a semidetached binary system. The second one is an interaction of stellar wind blowing from the mass losing star with another star. The third example is a mass loss from a contact binary system. Finite difference schemes are used to calculate gas flows. In either cases shock waves are formed because of gravitational focusing effect.

1. INTRODUCTION

Universe is generally supposed to be a vacuum, but this is not the case at all. Universe is entirely full of gases. Stars are made from gases, and spaces in between stars are filled by interstellar gases, which sometimes form massive interstellar clouds. Galaxies are agglomeration of stars and interstellar clouds, while these galaxies gather together to form larger system, cluster of galaxies. In clusters intracluster gas fills up the space between galaxies. Therefore gas dynamic technique are very useful in the research of the universe.

In the present review, examples of numerical simulation of cosmic gasdynamics, in which I and my colleagues are involved, are presented. The examples are the gas flow in close binary stellar systems.

In the binary system two stars revolve around their common centre of gravity. Binary stars are not exceptional, but almost half of stars in the galaxy are supposed to be members of binary systems. Interesting phenomena occur in close binary stars in which two component stars are so close that hydrodynamical interaction is expected to occur.

Gas is sometimes ejected from one component star, and phenomena such as X-ray emission occurs. Here I want to show the results of hydrodynamic calculation of gas flow in a semidetached binary system, in which one star fills its own Roche lobe, and also a contact binary system, in which two component stars fill their Roche lobes and therefore contact with each other.

2. BINARY SYSTEM

2.1 Classification of binary systems

As is noted in the introduction, binary stars are not exceptional but very common in the galaxy. The separation of two component stars ranges from order of kilometers to

* Department of Aeronautical Engineering, Kyoto University

order of light years, and therefore the revolution periods ranges from few minutes or even seconds to more than thousands years.

However it is not appropriate to talk about the closeness of two component stars in terms of separation, since radius of stars also ranges from few kilometers to the order of earth's orbital radius. Here it is useful to introduce the notion of Roche potential, which is produced by the gravitational force due to two mass points revolving around the common center of gravity, and also by the centrifugal force due to the rotation of the reference frame. Fig. 1 shows a cross-sectional view of Roche potential cut at the rotational plane. In the Roche potential there are five neutral points, at which force vanish, and they are denoted by L1 to L5. Although these points are generally called Lagrangian points, L1 to L3 points were firstly noted by Euler (Kozai, 1984 private communication).

The iso-potential surface, which goes through L1, is called Roche lobe and has a particular significance in considering binary stars. If a particle is inside one part of Roche lobe, the particle is said to belong that particular star. On the other hand, if the particle is outside of the Roche lobe, then the particle does not belong to a particular star, but is under the influence of both stars.

If the surfaces of two component stars are inside of Roche lobe, then this binary system is called a detached system. If a component star is big enough to fill the Roche lobe, then the system is called a semi-detached system. When both components fill the Roche lobe, the system is called a contact system (Kopal, 1955).

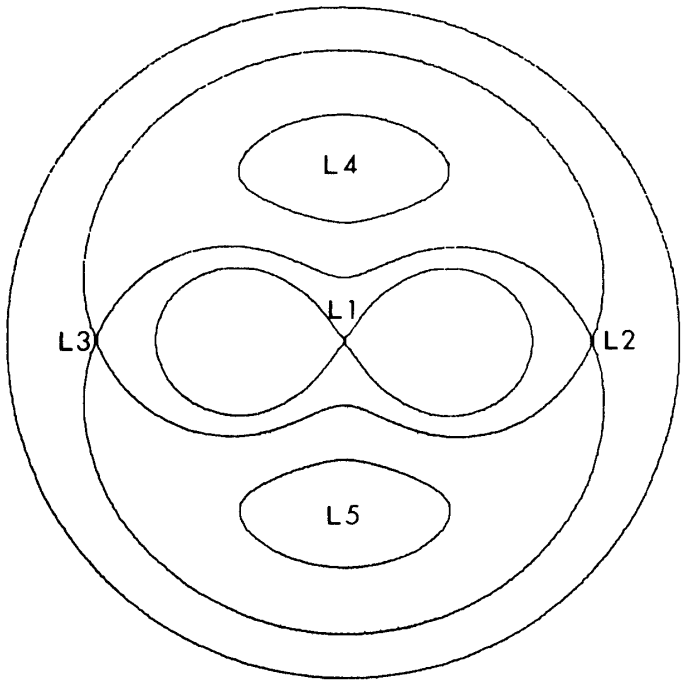

Fig. 1. The Roche potential produced by the combination of the gravity due to two revolving mass points, whose mass ratio is unity, and the centrifugal force. The points L1 to L5 are so called Lagrangian points where force vanishes. The eight shaped line shows the boundary of Roche lobe.

2.2 Evolution of binary system and the Roche lobe overflow

As stars evolve from main sequence stage, at which hydrogen burns at the centre, to giant stage, at which hydrogen shell burning or helium burning at the centre occurs, the stars expand. Since a more massive star evolves more quickly, the more massive component of binary stars may eventually fill the Roche lobe, and the binary starting as a detached system becomes a semi-detached system.

Further expansion of the more massive component induces a flow from the star surface to the territory of the other star through L1 point. This flow is called the Roche lobe overflow. Evolutionary scenario is in fact much more complicated, and the Roche lobe overflow occurs also in other occasions.

In any rate such Roche lobe overflow causes very interesting phenomena in astrophyscs. If the other star is not big, the gas ejected from the mass losing star is believed to form a disk surrounding the mass gaining star; it is called an accretion disk. If the mass gaining star is compact enough, then the disk becomes very hot due to the gravitational energy release and emit radiation such as X-ray, and the star is observed as X-star.

When the other component star evolves to fill its own Roche lobe, then the system becomes contact. Contact binary systems also pose interesting hydrodynamical problems.

3. Roche Lobe Overflow (Sawada, Matsuda & Hachisun, 1984)

Since Roche lobe overflow is very important phenomena in binary studies, lots of workers have investigated it so far. Early contributions were calculations of free particle trajectories. Since mean free path of gas is much shorter than the typical length scale, free particle approximation is irrelevant.

Biermann (1971) computed the stellar wind, which will be discussed in the next section, using the method of characteristics. Prendergast & Taam (1974) considered the case in which the mass accreting star is large. Sorencen, Matsuda & Sakurai (1975), Flannery (1975), Lin & Pringle (1976) and Hensler (1982) tried to investigate the case of a compact star. Method applied by Sorensen *et al.* and Flannery is finite difference methods, while Lin & Pringle and Hensler used particle techniques. Their method of solution are not sophisticated from the view point of modern computational fluid dynamics (CFD). In the present section, I introduce our resent work using generalized curvilinear coordinate and modern techniques of CFD.

3.1 The model

The star losing mass fills its own Roche lobe, while the mass gaining star is assumed to be compact. The density of gas at the surface of the mass losing star is specified, and is set to be unity in the nondimensional calculation. The sound speed of gas, which representes the internal energy of ejected gas, at the surface is also specified, but this is a parameter to be varied in the present study.

The gas is assumed to be ejected perpendicularly to the surface of the star. If the mass

loss is supersonic one at the surface of the star, one must specify the speed of gas, too. On the other hand, if the mass loss is subsonic one, one can not specify the speed of gas and it should be determined in the course of calculation. I mainly concern the subsonic case in this section. On the surface of the mass gaining star, all gas arriving on it is assumed to be absorbed.

I assume the whole process to be adiabatic except a shock heating, and neglect possible heating of gas by the illumination from the compact star, and neglect possible radiative coolings. This later assumption may be problematic, since the accretion disk is known to emit intense radiation. Nevertheless I assume this in order to make the whole problem nondimensional and to treat any binaries with any mass scale. In order to simulate the effect of cooling somehow, I compute the case with lower ratio of specific heats.

I also neglect viscosity in the computation. Viscosity is considered to be important for the gas in the accretion disk to accrete on the compact star by transffering angular momentum outwards. However it is very difficult to estimate the amount of realistic viscosity taking into account of turbulence and magnetic fields. Since our method of computation is the Osher upwind scheme which is first order accurate in space and in time, some diffusive effect is inherent in the computation. Such numerical diffusive effect would work as a model of realistic viscosity.

I restrict the computational domain within the rotational plane; gas is assumed to have a constant thickness in order to make the computation two dimensional. This simplification is justified if we restrict our attention within the region very close to the rotational plane.

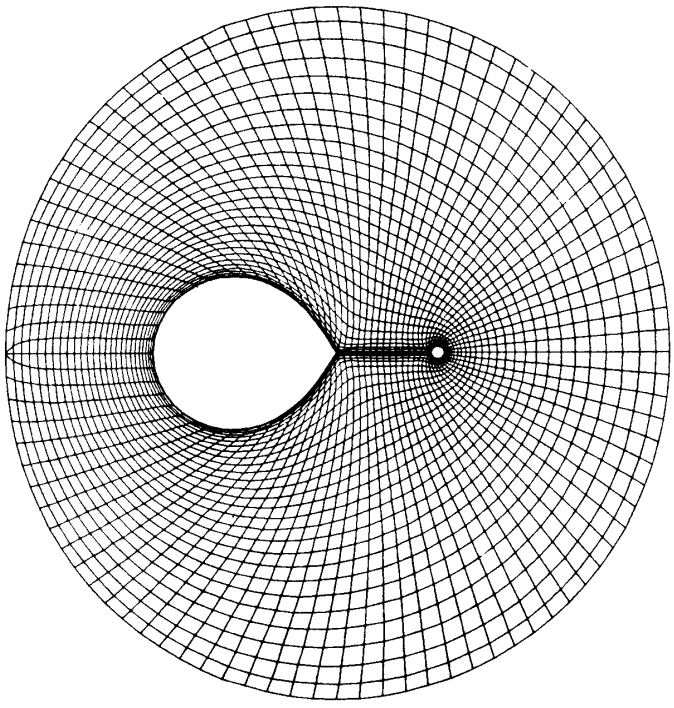

Fig. 2. Body fitted generalized curvilinear coordinate system. Number of meshes is 85×28.

On this two dimensional plane a body fitted coordinate shown in the Fig 2 is constructed. This computational domain is wide enough to treat possible mass loss from the binary system, and is fine enough to compute a complex flow around the compact star.

3.2 Basic equations

Let us introduce the generalized curvilinear coordinate (ξ, η) related to the Cartesian coordinate (x, y) by the relation:

$$\xi=\xi(x, y), \quad \eta=\eta(x, y). \tag{3.1}$$

The Jacobian, J, of this transformation is

$$J=\xi_x\eta_y-\eta_x\xi_y, \tag{3.2}$$

and the quantities called metric are defined as

$$\xi_x=Jy_\eta, \quad \xi_y=-Jx_\eta, \quad \eta_x=-Jy_\xi, \quad \eta_y=Jx_\xi. \tag{3.3}$$

The Euler equations describing the two dimensional time dependent flow written in the generalized curvilinear coordinate rotating at the binary orbital frequency are

$$(\partial U/\partial t)+(\partial F/\partial\xi)+(\partial G/\partial\eta)+H=0, \tag{3.4}$$

$$\begin{aligned} U&=J^{-1}\begin{pmatrix}\rho\\ \rho u\\ \rho v\\ e\end{pmatrix}, \quad F=J^{-1}\begin{pmatrix}\rho U\\ \rho uU+\xi_x p\\ \rho vU+\xi_y p\\ (e+p)U\end{pmatrix},\\ G&=J^{-1}\begin{pmatrix}\rho V\\ \rho uV+\eta_x p\\ \rho vV+\eta_y p\\ (e+p)V\end{pmatrix}, \quad H=J^{-1}\begin{pmatrix}0\\ \rho k_x\\ \rho k_y\\ \rho(uk_x+vk_y)\end{pmatrix}, \end{aligned} \tag{3.5}$$

where ρ represents the density, u and v the velocity components in the Cartesian coordinate, p the pressure, e the specific total energy, κ_x and κ_y the x and y component of the Roche force, U and V the contravariant velocity components along the ξ and η coordinate lines. These are related to the ordinary velocity component u and v through the following relation:

$$U=u\xi_x+v\xi_y, \quad v=u\eta_x+v\eta_y. \tag{3.6}$$

The x and y components of force are

$$\kappa_x = -2v - x + \frac{(\zeta/1+\zeta)}{r_1^3} x_1 + \frac{(1/1+\zeta)}{r_2^3} x_2,$$
$$\kappa_y = 2u - y + \frac{(\zeta/1+\zeta)}{r_1^3} y_1 + \frac{(1/1+\xi)}{r_2^3} y_2, \tag{3.7}$$

where ζ is the mass ratio of two stars, which is fixed to unity in the present work, $r_i (i=1, 2)$ the distance to the centre of each component star, x_i and y_i the coordinate component of r_i. In Eq. (3.7) the first terms of R.H.S. represent the Coriolis force, the second the centrifugal force due to the rotation of the reference frame, the third and the fourth the gravity due to each component star.

I assume the gas to be ideal one with the ratio of specific heats γ and, therefore the equation of state is written as

$$p = (\gamma - 1)(e - 0.5\, x(u^2 + v^2)). \tag{3.8}$$

In the present work I mainly consider the case of $\gamma = 5/3$, but the case with lower γ is also considered to take into account of cooling effects.

The equations are made dimensionless by adopting the separation of two stars, A, as the length scale, the Ω^{-1} as the time scale, the surface density of the mass losing star as the density scale.

3.3 Method of solution

The basic equations described above are solved by Osher's upwind finite difference scheme (Chakravarthy & Osher 1983, Osher, 1983). In aerodynamic problems, the most widely used method would probably be the Beam the Warming implicit scheme (Beam & Warming, 1976), which has second order accuracy in space compared to the first order accuracy of the Osher scheme. In the computation of the flow in the contact binary system, which will be described later, I apply the Beam-Warming method. However, in the present problem, the topology of the system considered is triply connected, and I need two cuts in space to map the phsical plane onto the singly connected computational plane. It is not a very easy task to handle the periodicity condition on the cuts properly in implicit methods.

Therefore, in the present problem, I employ an explicit scheme. Among various explicit schemes, the Osher scheme, which is an simplified version of Godunov scheme (Godunov, 1959), is known to be very robust. It can handle very strong shock waves and very sharp pressure contrast stably, because it does not show any wiggles, which are characteristic to most higher order schemes such as Mac-Cormack method, near discontinuities. In the following I shall explain Pandolfi's (1983) version of Osher scheme in physical terms.

Consider an one dimensional Euler equation written in a divergence form

$$U_t + F_x = 0, \tag{3.9}$$

which can be discretized as follows

$$(U_i^{n+1}-U_i^n)/\Delta t+(F_{i+1/2}^n-F_{i-1/2}^n)/\Delta x=0. \tag{3.10}$$

Now the problem is how to evaluate the flux $F_{i+1/2}$ at the intermediate position $x_{i+1/2}$. Since physical variables are defined at only integral points x_i, *it is plausible to define* $F_{i+1/2}=0.5(F_i+F_{i+1})$. This is a usual central difference scheme, but it is known to be unstable.

There is a more sophisticated way. Let us model the flow at time t^n with uniform flow U_i in the first half-interval $(x_i, x_{i+1/2})$ and uniform flow U_{i+1} in the second half-interval $(x_{i+1/2}, x_{i+1})$; such a procedure is called piecewise constant. A discontinuity is separating the two half-intervals and located at the mid point $x_{i+1/2}$.

Let us consider an evolution of this discontinuity (Riemann problem). As can be seen in Fig. 3, three characteristic waves corresponding to three eigenvalues $u-c$, u, $u+c$, where c is the sound wave, emerge. The waves $u-c$ and $u+c$ represent either shock wave or expansion wave while the wave u does a contact surface. The interaction between two uniform regions (U_i and U_{i+1}) generates two further uniform regions ($U_{i+1/3}$ and $U_{i+2/3}$). In the case shown in Fig. 3, where the waves $u+c$ and u propagate to the right, while $u-c$ propagates to the left, the flux at the mid point may be evaluated from $U_{i+1/3}$.

The exact solution of the Riemann problem invlolves a computational effort with iterative procedures because of possible shock. Instead of solving the Riemann problem exactly, Osher approximated the shock by a simple wave, and can solve it easily. Such an approximation is justified by numerical experiments.

The algorithm employed is a little bit more complicated than stated above, because

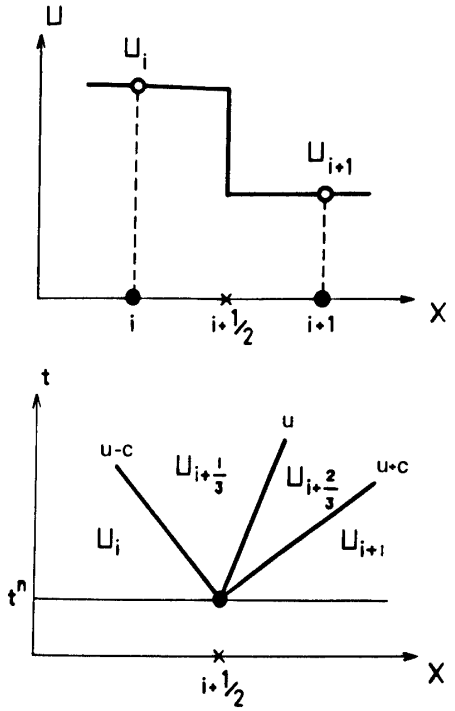

Fig. 3. 3 Illustration of the Riemann problem used in the Osher scheme.

expansion wave is not a line shown in Fig. 3 but a fan. If the head of the expansion wave runs left whereas the tail runs right, there is a sonic point, i.e. $u=c$, between the head and the tail. Such cases are treated properly in the Osher sheme.

3.4 Boundary conditions and an initial condition

The boundary conditions at the surfaces of the stars are discussed earlier. The algorithm to treat the surface boundary is different from Osher's (1983). Let us explain in the one dimensional case. At the surface, x_0, all components of U_0 is specified. Since U_1 is known, I can solve the Riemann problem to decide intermediate values $U_{1/3}$ and $U_{2/3}$. If all waves run right (outwards), which is a supersonic outflow case, U_0 is adopted as the boundary value to determine $F_{1/2}$. If waves travel as is shown in Fig. 3, which is a subsonic outflow case, $U_{1/3}$ is used as the boundary value. In the present study, ρ_0 is specified as unity, u_0 as a very small value and c_0 is a free parameter to be varied.

As to the boundary condition of the outer numerical boundary, I extrapolate physical variables from inner mesh points. I compute the steady state by the marching method, i.e. the steady state is obtained by following the time evolution of the system starting from some initial condition. Since Eulerian method of numerical hydrodynamics can not treat vacuum, I assume the existence of very thin gas everywhere at the initial time. The density of this gas is set to be as low as 10^{-5}, while the temperature of the gas is 10 times

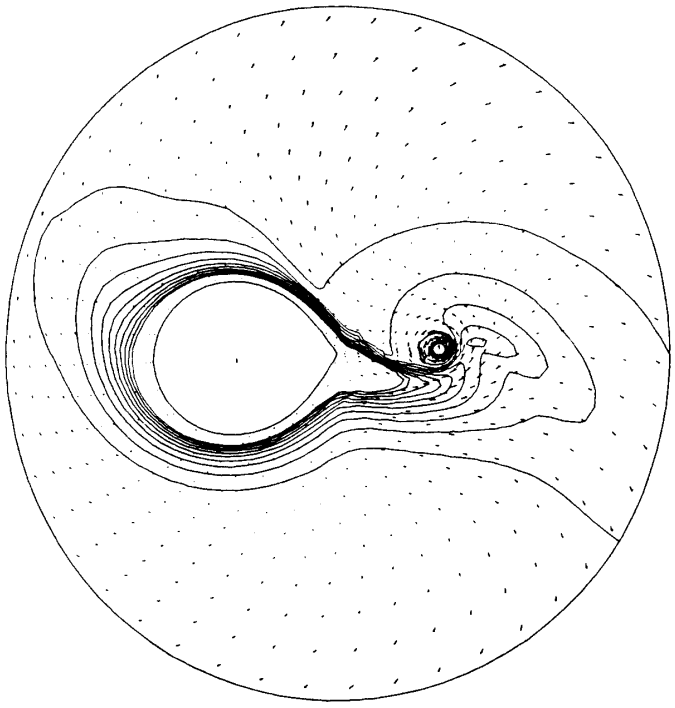

Fig. 4. Density and velocity distribution of final steady state of a Roche lobe overflow calculation. The iso-density lines range from 0.05 to 0.005. Velocity vectors are shown every each four cells. Shock can be observed at three to four o'clock direction of the compact star. Density enhancement at the tip of 'elephant trunk' is caused by the shock. Near the compact star desity is lower compared with outside, and accretion ring is formed.

higher than the surface temperature. Such gas is expelled from the computational domain in the course of evolution and does not give any effect on the final result.

3.5 Results

Fig. 4 shows a density distribution of a steady state. The sound speed at the surface of the mass losing star is set to be 0.3. As can be seen from the figure, gas ejected from the mass losing star mainly goes through L1 point to form an 'elephant trunk' like density enhancement. Gas leaving L1 point, which works as a Laval nozzle, soon becomes supersonic. The gas cannot hit the compact star directly because of the Coriolis force, and it produces a shock wave at three to four o'clock direction of the compact star. This shock is formed because of non-axisymmetric nature of the potential, and similar shocks are observed in the results described later. This shock is characteristic to the present calculation, and has not been observed in other works.

Behind the shock the gas is heated up, and a part of gas goes round the compact star to be absorbed ultimately by it, while the rest is reaccelerated to escape from the system. The leading hemisphere of the compact star becomes very hot (the system rotates counter clock wise.). Around the compact star is almost vacuum and an accretion ring rather than an accretion disk is formed, because gas next to the star is absorbed but the supply is short.

The reason for this short supply is a lack of angular momentum transport outwards in the accretion ring; the transport is probably caused by turbulent and/or magnetic viscosity in the real system. In the present algorithm an artificial viscosity is absent, but a numerical diffusion inherent in the algorithm works as the viscosity. Therefore the mesh size can be considered as a mixing length. Generally the existence of the accretion disk is believed, and the elephant trunk is believed to hit with the disk to form a shock at say seven o'clock. Such a picture is not confirmed in the present work.

Observing Fig. 4, one can see that almost gas ejected from the mass losing star escape from the system rather than accreted on the compact star. The route of the escape is twofold. One is through L2 point, and the other is through L3 point. Other researchers (Lin & Pringle 1975, Hensler 1982) insist that almost of ejected gas, say 97 percent, is ultimately accreted onto the compact star. Our present calculation does not predict this. This is partly due to the insufficient angular momentum transfer.

Another factor to be considered is a pressure behind the shock. One may say that if I include the effect of cooling, then almost gas would be absorbed. I examine the case by reducing the ratio of specific heast as low as 1.1. In this case the density enhancement behind the shock becomes high, while the temperature and pressure rise is kept mild. The result is, however, very similar to the higher γ case.

In order to reduce the temperature of gas, the case with low sound speed at the surface of the mass losing star, i.e. $c_0=0.03$, is computed. The result shows that the absolute value of density of gas is much lower than the case described above, but it is found that the density pattern is essentially same as before.

4. Formation of Accretion Shock Behind a Star (Shima, Matsuda, Takada & Sawada, 1984)

Fig. 5 shows the density distribution of the case in which the sound speed of the ejected gas is 5; very hot gas is ejected. The gas becomes supersonic all over the mass losing star quickly, and becomes stellar wind. The wind interact with the compact star, and an accretion shcok is formed behind the star. Although similar calculation was performed by Biermann (1971), he could not compute shocks because his method assumed everywhere to be supersonic. In front of the compact star gas is accelerated towards the star, and the low density region is formed.

This result is obtained by assuming the constant thickness of gas. However, in the present case, gas would be ejected almost isotropically, and therefore three dimensional effect can not be neglected. In order to see this effect, I carry out another simulation in which a star is immersed in a uniform hypersonic flow. Under such an assumption, I can assume axisymmetry and computations are considerably simplified.

This class of accretion problem has long history (Eddington, 1926; Hoyle & Lyttleton, 1939; Bondi, 1952). Hunt (1971) was the first to study the problem numerically. He used Lax-Wendroff method in a quite tricky way. He could not obtain stable solutions by simply adding artificial viscosity, and therefore he assumed that entropy should be constant except shocks and density should be larger than unity, i.e. the density at

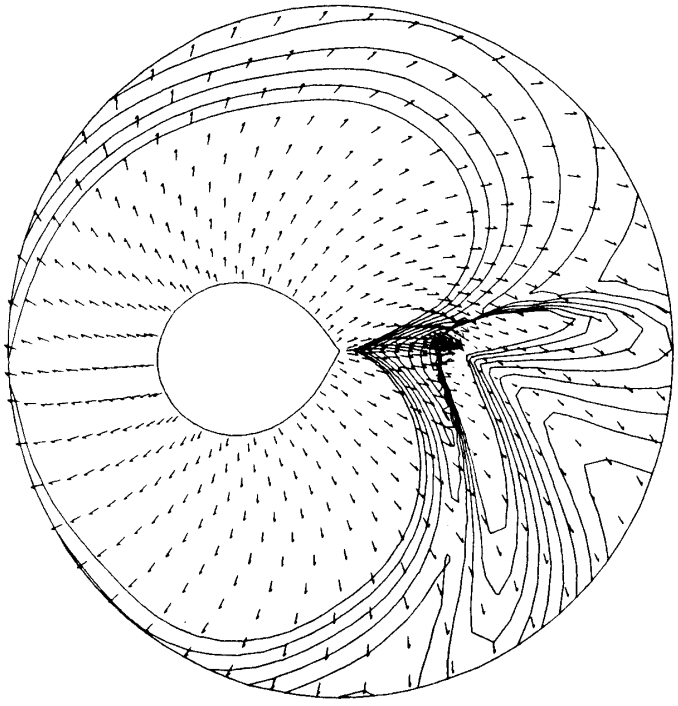

Fig. 5. Density and velocity distributions in a stellar wind interacting with a compact star. Iso-density contours ranges from 0.1 to 0.05. The density minimum occurs in front of the compact star. Accretion shock is formed behind the compact star. The maximum Mach number, which occurs at the head of the compact star, is 4.

infinity. Although such assumptions could not be justified a priori, his solution seemed to be quite reasonable. He computed the flows with Mach number only up to 2.4.

Shara & Shaviv (1980) computed the flow past a rigid body; their Mach number was as large as 14.8. Takeda, Matsuda, Sawada & Hayashi (1984) studied the viscous flow past a rigid body to compute the drag coefficient. The method is Beam & Warming implicit one. The Mach number is up to 2, and the Raynolds number is 10 to 40. In the following, I show recent results of calculation of hypersonic flows using the Osher scheme. Basic equations are rewritten in axisymmetric coordinate.

Let us consider a sphere placed in gas of which velocity and density are uniform at the far upstream. If viscosity and gravity are neglected, a relevant parameter characterizing the flow is Mach number. Fig. 6 shows a density contour of such flow with Mach number $M=14.8$. The sphere is assumed to be rigid, and the boundary condition at the surface is slippery one. As can be seen in the figure, an intense bow shock is formed in front of the sphere.

Now let us introduce the gravity. As to the surface boundary condition, I consider two extreme cases: slippery condition and completely absorbing condition.

When gravity is taken into account, a new parameter describing the system is introduced. Let us define an accretion radius r_a as $r_a=2Gm/u_0^2$, where G is the gravitational constant, m the mass of the star and u_0 the gas speed at infinity. A relevant nondimensional parameter is the ratio of the accretion radius to the radius of the star, r. I call it δ following Ruderman & Spiegel (1971), and it is defined as

$$\delta=r_a/r, \tag{4.1}$$

Fig. 7 shows the density distribution around a completely absorbing star; the boundary

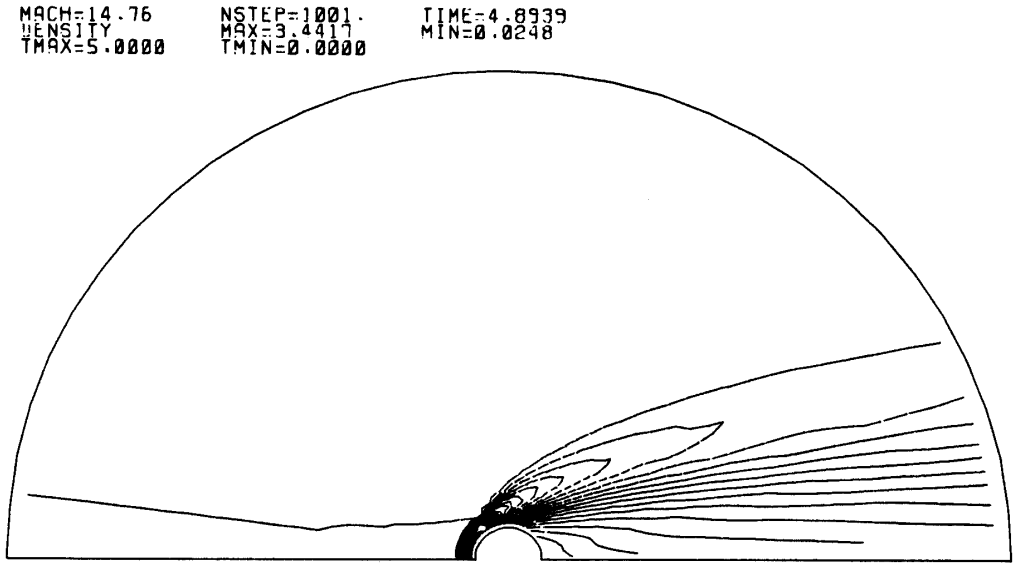

Fig. 6. The density distribution in the flow interacting with a solid slippery sphere. Mach number of the uniform flow at the far upstream is 14.76. The maximum and minimum of the density are 3.4417 and 0.0248. The maximum occurs at the head and the minimum does at the back side of the sphere. The iso-density contours ranging from 0 to 5 are displayed. A bow shock is observed.

condition on the star is that of very low pressure and density as was assumed by Hunt (1971). The parameter δ is 4 in this model. A straight shock attached to the star is clearly observed. Hunt considered the case in which the accreting star was infinitesimally small, i.e. very large δ, and concluded that the shock originated in front of the star, i.e. a bow shock. Since size of our star is larger than Hunt's, it is not seen in the present model. By increasing δ, I confirm Hunt's result. In any rate the shock pattern does not agree with one predicted by Ruderman & Spiegel (1971), who considered that the shock was a detached cone originating at the downstream of the star.

It should be noted that the angle of the shock cone is different from a Mach angle. This

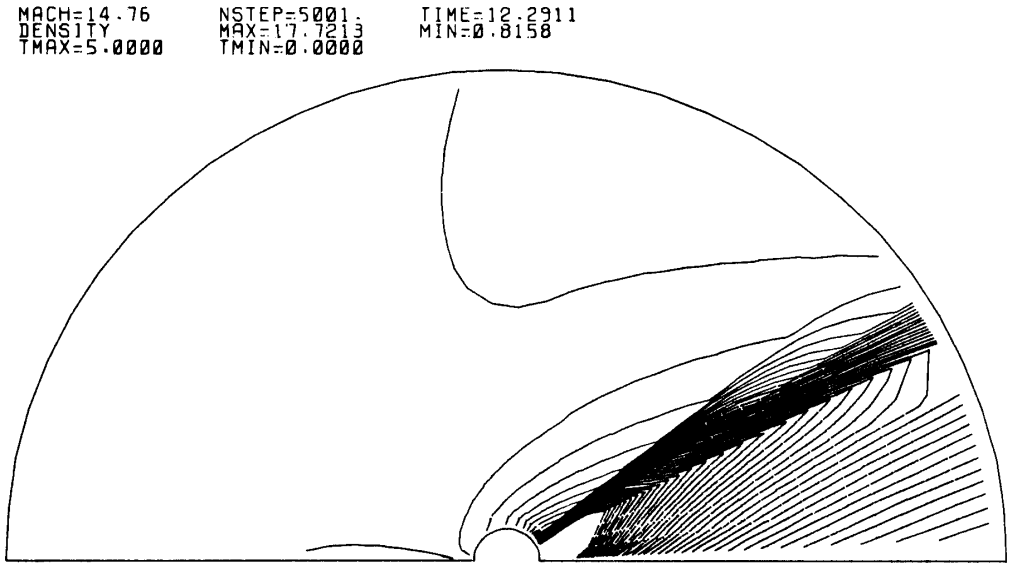

Fig. 7. Density distribution of the flow interacting with a absorbing gravitating sphere. An accretion radius is four times of the radius of the sphere. An intense accretion shock is formed. The maximum of the density occurs at the back side of the sphere. Other nomenclator are the same as Fig. 6.

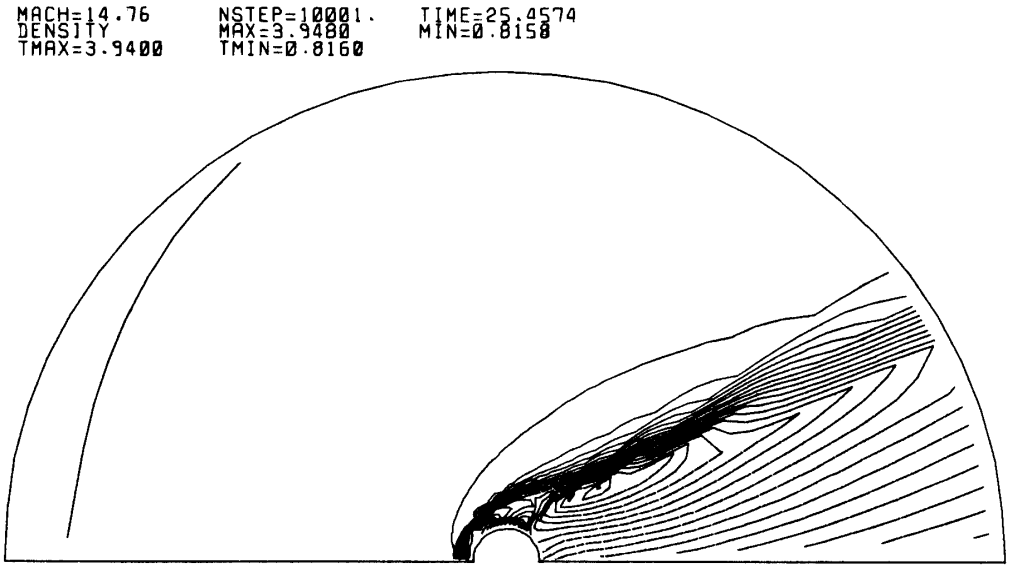

Fig. 8. Same as Fig. 7 except that the sphere's surface is slippery.

shock is not caused by the direct interaction between the flow and the star, but by the gravitational focussing effect. Therefore this angle does not vanish even at the limit of infinitely large Mach number.

An interesting point to note is that the density has a ridge on the shock cone. Therefore it may not be appropriate to call it the accretion column as is called commonly, but is better to call it an accretion cone.

Fig. 8 shows a similar case as before, but the surface of the star is assumed to be slippery as was assumed by Shara & Shaviv (1980). Two types of shock, i.e. a bow shock ahead of the star and an accretion shock behind of the star, are observed. However, as far as a distant region is concerned, the density pattern is almost same as Fig. 7. Therefore it can be concluded that the far flow is not very affected by the syrface boundary condition. Note that the present flow pattern is very different from Shara & Shaviv's, which does not show any shock like features in spite of large Mach number. They are probably smeared out by large artificial viscosity.

5. Mass Loss from a Contact Binary System (Sawada, Hachisu & Matsuda, 1984)

If the binary system is contact, the gas ejected, if any, from a star can not be absorbed by the other star. The reason is that a time scale for a star to absorb gas accreted on it is a thermal time scale which is much longer than a dynamical time scale considered. Therefore it may be appropriate to assume the surface boundary condition of the other star to be one of slippery.

Now let us show an example of mass loss from a contact binary system. Method of computation is the Beam and Warming implict scheme. The Fig. 9 shows the density distribution of gas and the velocity vector seen on the inertial frame rather than the rotational frame. Mach number distribution and the velocity vector seen on the rotational frame are shown in Fig. 10. The inner most line is the sonic line.

Part of gas ejected from the lefthand star leaves the system through L3 point to from a characteristic spiral pattern, and the rest of gas goes around the righthand star to escape the system through L2 point. As can be seen in Fig. 10, the speed of gas is at first subsonic, and is accelerated to become supersonic. Such an acceleration is observed in our solar wind as well.

Interesting point to note in Fig. 10 is that shock waves are formed at the leading side of the spiral arms. (The system rotates counter clock wise.) Non-axisymmetry of the flow, which is induced by the non-axisymmetry of the force, causes the shock. In the inertial frame it can be explained as a faster stream catches up slower stream, and a collision occurs between streams (see Fig.9).

A siginificance of this sort of simulation is to compute the angular momentum loss rate from the system. By loosing mass, the system loses angular momentum as well. If the specific angular momentum loss is larger than the specific orbital angular momentum, the system shrinks as a whole. If this shrinking is fast enough, the system will finally merge to form a single star. Whether this happens or not is an important problem in the theory of binary star evolution. In the present calculation this quantity is evaluated as 1.65 in non-dimensional unit, which does not contradict wiht a result based on a particle

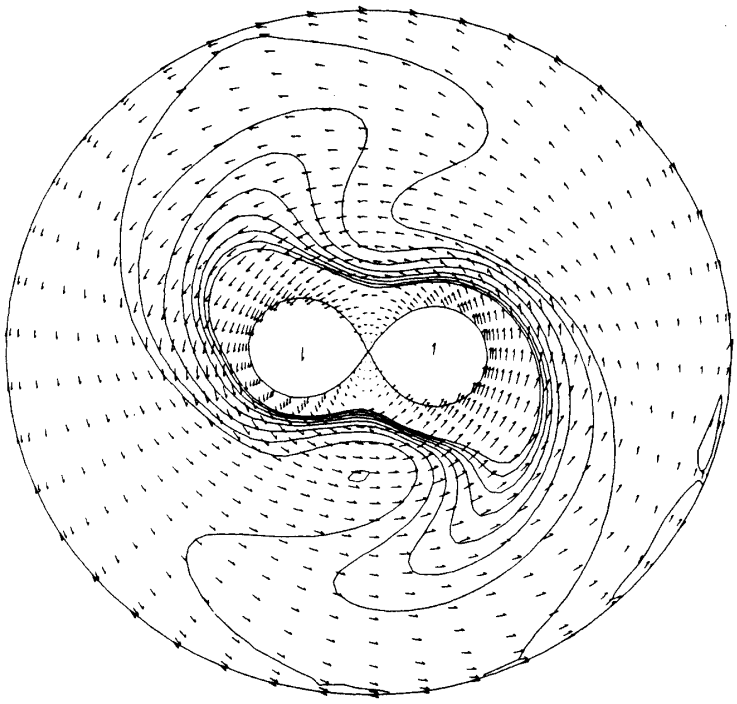

Fig. 9. Density distribution of the flow in a contact binary system. Velocity is seen in the inertial frame. The arrows in the stars show the sense of rotation as well as unit magnitude of the speed.

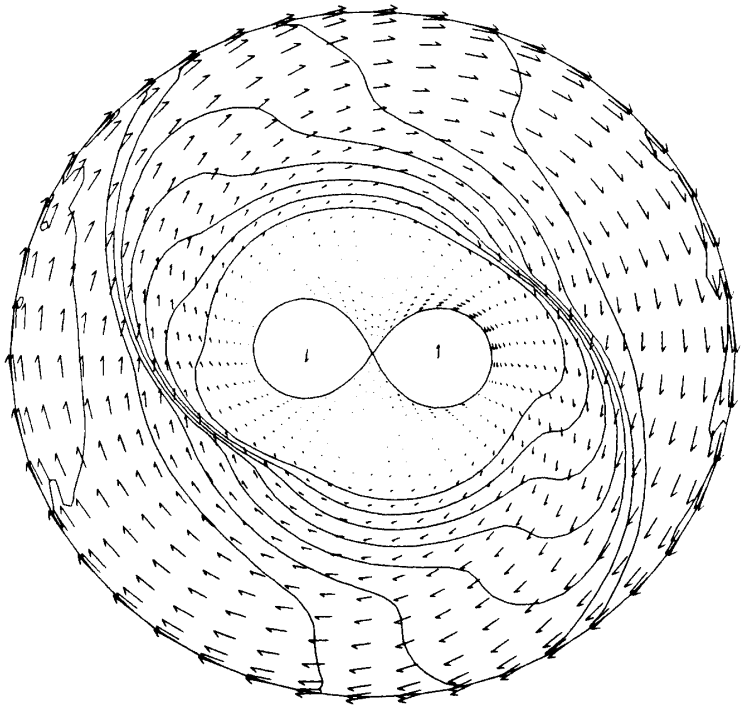

Fig. 10. Iso-Mach number lines ranging rom 1 to 5. The innermost line shows a sonic line. Velocity is seen in the rotating frame.

calculation (Nariai, 1976). However, it should be stressed that the gas obtain angular momentum abruptly by going through shocks. It is not a gradual process as is in the case of particle calculations.

Acknowledgement

The works presented in this paper have been done in a collaboration with Dr. H. Takeda, Dr. I. Hachisu, Mr. K. Sawada and Mr. E. Shima. I am grateful for their cooperation. The computations have been performed by Fujitsu VP100 vector processor and M382 at the Data Processing Centre of Kyoto University, and by M380 at the Institute of Space and Astronautics Science, and by M200 at the Nobeyama Radio Observatory. This research was supported by the Grant-in-Aid for Scientific Research (59540155) of the Ministry of Education, Science and Culture in Japan.

References

[1] Beam, R. M. and Warming, R. F.: J. Comp. Phys. *50*, (1976) 447.
[2] Biermann, P.: Astron. Astrophys. *10*, (1971) 205.
[3] Bondi, H.: Mon. Not. R. astr. Soc. *154*, (1952) 141.
[4] Chakravarthy, S. R. and Osher, S.: AIAA J. *21*, (1983) 1241.
[5] Eddington, A. S.: The Internal Constitution of the Stars, pp. 391–393, Cambridge Univ. Press, (1926).
[6] Flannery, B. P.: Astrophys. J. *210*, (1975) 661.
[7] Godunov, S. K.: Matematicheskii Sbornik *47*, (1959) 271
[8] Hensler, G.: Astron. Astrophys. *114*, (1982) 309.
[9] Hoyle, F. and Lyttleton, R.: Proc. Camb. Phil. Soc. *35*, (1939) 405.
[10] Hunt, R.: Mon. Not. R. astr. Soc. *154*, (1971) 141.
[11] Kopal, Z.: Ann. Astrophys. *18*, (1955) 371.
[12] Lin, D. N. C. and Pringle, J. E.: IAU Symp. *73*, (1976) p237.
[13] Nariai, K.: Astron. Astrophys. *43*, (1975) 309.
[14] Osher, S.: J. Comp. Phys. *50*, (1983) 447.
[15] Pandolfi, M.: AIAA J. *22*, (1984) 602.
[16] Prendergast, K.-H. and Taam, R. E.: Astrophys. J. *189*, (1974) 125.
[17] Ruderman, M. and Spiegel, E. A.: Astrophys. J. *165*, (1971) 1.
[18] Sawada, K., Hachisu, I. and Matsuda, T.: Mon. Not. R. astr. Soc. *206*, (1984) 673.
[19] Sawada, K., Matsuda, T. and Hachisu, I.: Work in progress, (1984).
[20] Shara, M. M. and Shaviv, G.: Astrophys. Space Sci. *67*, (1980) 427.
[21] Shima, E., Matsuda, T., Takeda, H. and Sawada, K.: Work in progress, (1984).
[22] Sorensen, S.-A., Matsuda, T. and Sakurai, T.: Astrophys Space Sci. *33*, (1975) 465.
[23] Takeda, H., Matsuda, T., Sawada, K. and Hayashi, C.: Submitted for publication, (1984).